Indian Journal of Fibre & Textile Research
Vol. 51, March 2026, pp. 53-66
DOI: 10.56042/ijftr.v51i1.14191

Mathematical modelling and improved control system for reducing warp yarn tension fluctuation in sizing machines

Li Tu[1,2], Mingrui Guo[1], Jingan Wang[1,a] & Weidong Gao[1,3,b]

[1]Department of Textile Science and Engineering, Jiangnan University, Wuxi 214 122, China

[2]School of New Materials and Shoes & Clothing Engineering, Liming Vocational University, Quanzhou 362 000, China

[3]Jiangnan University (Shaoxing) Industrial Technology Research Institute, Shaoxing 312 000, China

Received 5 October 2024; revised received and accepted 10 November 2025

In the sizing process, warp yarn tension often fluctuates when the residual yarn of the warp beam is approximately 35% of the full beam with a typical closed-loop tension control system. It affects sizing quality and the uniformity of the fabric's appearance. Therefore, this paper first establishes the theoretical models of the warp yarn unwinding process and tension control system to clarify the warp yarn tension fluctuations mechanism. Subsequently, control system improvement methods are proposed and verified through simulations based on these models, including the addition of an independent air pressure device and a segmented control approach. Finally, the rationality of the proposed models and methods are experimentally confirmed using the constructed detection devices. Simulation analysis revealed that constant tension system control parameters and uneven moment of inertia of the warp beam cause system oscillations and larger yarn tension fluctuations. By installing air pressure device and implementing segmented control, the yarn tension fluctuation range is reduced by 83.16% and 89.44% respectively. Additionally, experimental results further indicated that the proposed models and improved control system are effective. Thus, this paper provides a significant theoretical foundation and practical guidance for stabilising unwinding tension in sizing machines, with potential applications across the textile industry.

Keywords: Control system, Mathematical models, Sizing process, Unwinding tension, Warp yarn

1 Introduction

The uniformity and stability of warp yarn tension during the sizing process are essential for meeting the demands of weaving production[1-3]. Excessive warp yarn tension not only increases the risk of yarn breakage but also hinders the effective penetration of the sizing agent, directly impacting the production efficiency and quality of the sized yarn. Conversely, insufficient warp yarn tension can lead to loose yarn, resulting in uneven winding of the sized yarn on the weaver's beam[4,5]. Therefore, it is crucial to accurately control warp yarn tension during the sizing process.

In recent years, the radius and number of warp beams have been improved with the innovation of sizing machines[6-8]. However, the warp yarn unwinding tension control has always adopted a typical closed-loop tension control system. The warp yarn is unwound through a combination of passive warp beam delivery and friction braking of the warp beam[9,10]. In the actual sizing production, as the unwinding process proceeds, warp yarn tension often fluctuates due to various factors such as the warp beam's unwinding radius, moment of inertia, and the tension control system. Notably, these fluctuations become particularly serious when the residual yarn of the warp beam is approximately 35% of the full beam[11-13]. This phenomenon can negatively impact the sizing quality and the fabric's appearance uniformity during weaving. Additionally, tension fluctuations can also increase the amount of residual yarn, resulting in a waste of resources[14-16]. The amount of residual yarn after the unwinding in the denim product production workshop is shown in Fig. 1. Thus, the unwinding zone, as the first tension control zone of the sizing machine, is necessary to reduce warp yarn tension fluctuations.

There has been continuous research on the warp yarn tension of sizing machines. Zhang[17] combined theoretical and experimental research to explore the causes of uneven tension in wave-type and upward-pull-type unwinding methods for single-layer multi-warp beams. Similarly, Hu[18] studied the wave-type unwinding process, finding that the warp beams closer to the slurry tank experience greater tension. For double-layer multi-warp beam unwinding, Chen

[a]Corresponding author.
E-mail: wja1124@gmail.com, gaowd3@163.com

et al.[19] Tested the warp yarn tension of large warp beams on the Zucker sizing machine creel. Their results showed minimal differences in warp yarn tension and beam hardness for warp beams without overlapping winding. Furthermore, Ru *et al*.[20] measured the dynamic tension of high and low beam beams, and found that the warp yarn unwinding tension fluctuates periodically, which is particularly significant when the diameter of the warp beam decreases. Collectively, these studies highlight that warp yarn tension is influenced by various factors and that fluctuations persist during the unwinding process.

To address these tension fluctuations, researchers have proposed various warp yarn tension control methods[21-23]. Xue[24] integrated a tension sensor and a rotation speed encoder to monitor the warp beam unwinding speed, achieving constant warp yarn tension control. Next, Tong *et al.*[25] targeted warp warp yarn tension and elongation, using mechanical devices, electrical sensors, and PLC-controlled frequency converters for precise regulation. Moreover, Li *et al*.[26] and Liu *et al*.[27,28] applied a neural network and fuzzy PI control algorithm to adjust warp yarn tension, demonstrating efficient automatic control with good dynamic response, interference resistance, and accuracy. These methods represent advancements in tension control technology and address some of the problems identified in earlier studies.

Fig. 1 — The amount of residual yarn after the unwinding in the denim product production workshop

However, the mechanism of tension fluctuation when the residual yarn of the warp beam is approximately 35% of the full beam remains unexplored. Existing research has not proposed specific improvements for this critical unwinding stage. This phenomenon persists in actual production, impacting sizing quality, production efficiency, and residual yarn levels. Therefore, it is necessary to investigate and control this phenomenon to enhance warp yarn tension stability and improve sizing quality.

In this paper, we first establish mathematical models of the warp yarn unwinding process and tension control system to clarify the mechanism of warp yarn tension fluctuations. Subsequently, control system improvement methods for addressing these fluctuations are proposed and verified by simulations based on these models. These methods include the addition of an air pressure device and the segmented control method to decrease warp yarn tension fluctuations. Furthermore, the rationality of the established models and the effectiveness of the proposed improvement methods are experimentally verified using constructed detection devices for unwinding tension, speed, and radius. This paper provides a theoretical foundation and effective methods for maintaining stable yarn tension in the sizing process and across the textile industry, thereby enhancing both production efficiency and product quality.

2 Materials and Methods

2.1 Theoretical Models

2.1.1 Warp Yarn Unwinding Process

The warp yarn unwinding process in a sizing machine refers to the passive and synchronized unwinding of each warp sheet from its respective warp beam. In this zone, multiple warp beams and guide rollers work together, as illustrated in Fig. 2.

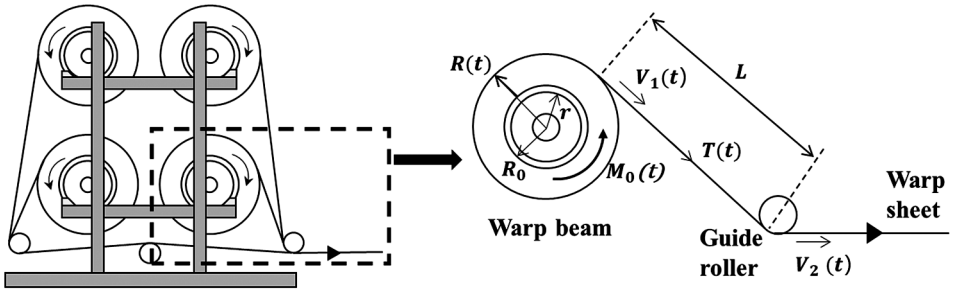

Fig. 2 — Schematic diagram of the warp beam unwinding zone

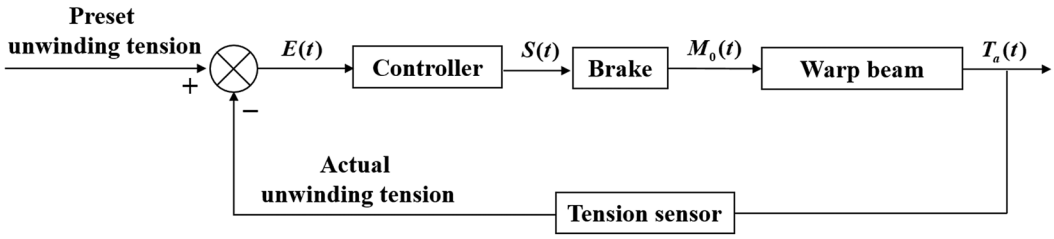

Fig. 3 — Closed-loop control system for warp yarn unwinding tension

The warp beam unwinding radius $R(t)$gradually decreases during the entire unwinding process, the change rate of $R(t)$ can be expressed as:

$$\frac{dR(t)}{dt} = -\frac{h}{2\pi}\frac{V_1(t)}{R(t)} \quad \ldots (1)$$

where h is the thickness of each warp yarn layer, $V_1(t)$ is the warp beam unwinding speed.

In general, the moment of inertia of the warp beam $J(t)$is composed of the empty warp beam and the yarn on the warp beam. Its variation over time t is given by:

$$\frac{dJ(t)}{dt} = \frac{1}{2}\pi b\left(R^4(t) - {R_0}^4\right)\frac{d\rho(t)}{dt} + 2\pi b\rho(t)R^3(t)\frac{dR(t)}{dt} \quad \ldots (2)$$

where,b is the distance between the flanges, $R_0$is barrel radius, $\rho(t)$ the warp beam winding density.

However, the warp beam may be eccentric due to wear, material fatigue or other factors in actual production. When an eccentric warp beam rotates, the imbalance of the circumferential force armwill make the radial forces inside the bearing to be unbalanced, which can further lead to uneven changes in the moment of inertia and oscillations in the system. This phenomenon is particularly obviouswhen the residual yarn of the warp beam is approximately 35% of the full beam. Therefore, in order to describe this phenomenon, an interference term $U(t)$is introduced:

$$U(t) = \lambda \sin\omega t \quad \ldots (3)$$

where, λ is the amplitude of interference, $\omega$is the frequency of the interference.

So, Eq. (2) can be further written as:

$$\frac{dJ(t)}{dt} = \frac{1}{2}\pi b\left(R^4(t) - {R_0}^4\right)\frac{d\rho(t)}{dt} + 2\pi b\rho(t)R^3(t)\frac{dR(t)}{dt} + \lambda\omega\cos\omega t \quad \ldots (4)$$

Based on Newton's second law of rotational motion, the dynamic moment equation of the warp beam unwinding process is:

$$T(t)R(t) - M_f(t) - M_0(t) = \frac{d(J\omega)}{dt} \quad \ldots (5)$$

where, $T(t)$is the unwinding tension of the warp yarn, $M_f(t)$ is the frictional resistance torque, $M_0(t)$ is the braking torque, $\omega(t) = \frac{V(t)}{R(t)}$ is the angular speed of the warp beam.

Specifically, the frictional resistance torque $M_f(t)$ is expressed as follows:

$$M_f(t) = \beta r\left[G_0 + \pi b\rho(t)\left(R^2(t) - {R_0}^2\right)\right] \quad \ldots (6)$$

where,β is the coefficient of friction, r is the ruffle radius, $G_0$is the weight of the empty warp beam.

Therefore, combining Eqs. (1), (4), (5) and (6), the coupling model between the warp yarn unwinding tension and various factors can be derived as:

$$T(t) = \frac{M_0(t)}{R(t)} + \frac{\beta r\left[G_0 + \pi b\left(R^2(t) - {R_0}^2\right)\rho(t)\right]}{R(t)} - hb{V_1}^2(t)\rho(t) + (K_1 + \lambda\sin\omega t)\left[\frac{1}{R^2(t)}\frac{dV_1(t)}{dt} + \frac{h{V_1}^2(t)}{2\pi R^4(t)}\right] + (K_2\frac{d\rho(t)}{dt} + \lambda\omega\cos\omega t)\frac{V_1(t)}{R^2(t)} \quad \ldots (7)$$

where, $K_1 = \frac{1}{2}G_0R_0^2 + K_2\rho(t), K_2 = \frac{1}{2}\pi b\left[R^4(t) - {R_0}^4\right]$.

Meanwhile, the warp yarn on the warp beam is analyzed according to the law of conservation of mass[29].The unwinding tension is generated by the speed difference between the guide roller and the warp beam, which is written as:

$$\frac{dT}{dt} = \frac{EA}{L}\left[V_2(t) - V_1(t)\right] - \frac{1}{L}T(t)V_2(t) \quad \ldots (8)$$

where,E and A are the elastic modulus and cross-sectional area of the warp yarn respectively, L is the distance between the warp beam and the guide roller, $V_2(t)$ is the guide roller speed.

2.1.2 Warp Yarn Unwinding Tension Control System

Based on the above models, it is found that the warp yarn unwinding tension control system of a sizing machine exhibits nonlinear and time-varying characteristics[30,31], and its schematic diagramis depicted in Fig. 3.The entire control system includes controller, brake, warp beam and tension sensor.

When there is a deviation $E(t)$ between the preset unwinding tension $T_p(t)$and the actual detected tension $T_a(t)$, the controller immediately generates the corresponding air pressure adjustment amount $S(t)$. Then, this adjustment modifies the braking torque $M_0(t)$applied by the brake to the warp beam, changing the unwinding speed of the warp beam.Consequently, the speed difference between the warp beam and the guide roller is altered, thereby adjusting the warp yarn unwinding tension.

The brake serves as the actuating element and can be regarded as a proportional component, whose transfer function is expressed as:

$$G_b(s) = K_3 \quad \ldots (9)$$

where,K_3 is proportional coefficient of the brake.

Meanwhile, the warp beam acts as the controlled object. Based on Eqs. (5), its corresponding transfer function can be derived as:

$$G_w(s) = \frac{R}{Js+\beta} \quad \ldots (10)$$

The tension is generated by the speed difference, and it is measured by the tension sensor. By combining Eqs. (8) and considering the tension sensor as a proportional component, its transfer function can be obtained as:

$$G_t(s) = \frac{K_4 K_5}{s+C} \quad \ldots (11)$$

where $K_4 = n\frac{EA}{L}$, nis the total number of warp yarns on the warp beam, $C = \frac{V_2}{L}.K_5$ is proportional coefficient of the tension measuring device.

Combining the transfer functions of the above components, the transfer function of the whole control system can be obtained as:

$$G(s) = G_b(s) \cdot G_w(s) \cdot G_t(s) = \frac{K_3 K_4 K_5 R}{Js^2 + (\beta + CJ)s + \beta C} \quad \ldots (12)$$

2.2 Simulation Analysis

The PID closed-loop tension control method is widely used in sizing machines due to its stability, reliability and relatively simple realization. The PID controller calculates the control quantity $S(t)$ based on the system error $E(t)$ through proportion, integration and differentiation. The specific control rules are as follows:

$$E(t) = T_p(t) - T_a(t) \quad \ldots (13)$$

$$S(t) = K_P\, E(t) + K_I \int_0^t E(t)dt + K_D \frac{dE(t)}{dt} \quad \ldots (14)$$

where K_P,K_I and K_D are the proportional gain, integral gain and derivativegain respectively.

However, the production experience has shown that with a typical closed-loop tension control system, warp yarn tension often fluctuates when the residual yarn of the warp beam is approximately 35% of the full beam. Therefore, based on theoretical models of the unwinding process and tension control system, the PID closed-loop control system is simulated to clarify the mechanism of tension fluctuations.

Subsequently, the following improvement methods are proposed, including adding the air pressure device to directly regulate the fluctuation of tension and the segmented control method for optimizing the control parameters of warp yarn tension control system to reduce the warp yarn tension fluctuation. Based on these theoretical models, the control effect of the proposed methods is further verified through simulation experiments.

2.3 Experimental Method

In actual sizing production, warp yarn tension fluctuations when the residual yarn of the warp beam is approximately 35% of the full beam are often reduced by decreasing the speed through operational experience. This is because a lower speed decreases the rotational speed of the warp beam, thereby weakening the inertial effect on tension. Therefore, based on the established model with the warp yarn unwinding process and tension control system, the method of speed reduction to reduce tension fluctuation is simulated to establish the relationship between the decreased rate of speed and tension fluctuations range. Then, the consistency of this relationship with the actual results is verified by constructing testing devices. Once the relationship between speed decrease rate and tension fluctuations change is proved, it validates the accuracy of theoretical model for the warp yarn unwinding process and control system. This further demonstrates the effectiveness and feasibility of the proposed improvement methods based on model simulations.

Detection devices were constructed to measure warp yarn tension, unwinding speed, and warp beam unwinding radius. Specifically, a resistance strain-type three-pulley tension sensor and an independently designed fixing device were utilized to measure the warp yarn tension with a detection range of 0-20 N.

During the unwinding process, multiple warp yarns on the beam are arranged in parallel and evenly distributed. Under the same driving force, the tension distribution of yarns on the left, middle, and right sides of the beam is theoretically consistent. Since the speed and radius detection devices were both installed on the left side of the warp beam, the tension of 10 yarns at the leftmost end of the warp beam was measured for convenience of operation and synchronized data acquisition, and their average value was obtained to determine the single warp yarn tension. The unwinding speed was measured using a speed sensor and a fixing device. The speed sensor, functioning on the principle of perimeter measurement, is a roller meter with a diameter of 64 mm. The ultrasonic distance sensor and the magnetic crab clamp meter base fixture were used to measure the warp beam unwinding radius. The distance to be measured is determined by measuring the time difference between transmission and reception of the ultrasonic wave. The detection range is 70-1000 mm. During measurement, it is crucial to ensure that the sensor is within its detection range and aligned with the warp beam axis. Additionally, an application that can simultaneously read the data of the above three sensors in real time was developed by Python and Modbus communication protocol. The serial port and baud rate of the corresponding sensors were matched to realize the reading and saving of data.

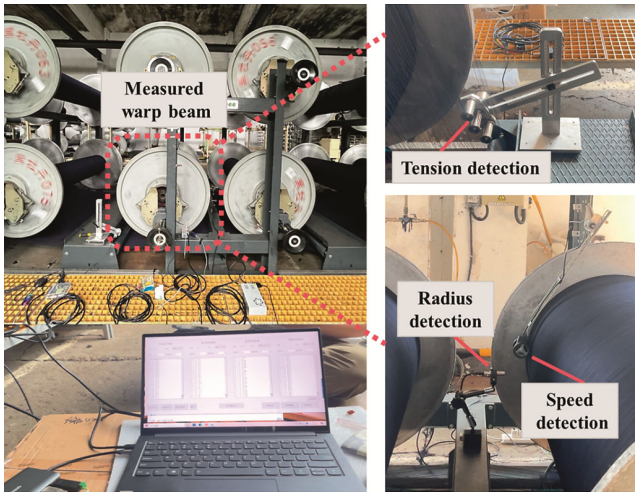

Fig. 4 — Physical diagram of the measured warp beam

Experimental tests were carried out on the warp beams mounted on the H-type creel of a Karl Mayer PROSIZE sizing machine in an actual sizing workshop. Fig. 4 shows the physical diagram of the warp beam measurement. Using the aforementioned detection devices and data reading software, the warp yarn tension, unwinding speed and warp beam unwinding radius changes of before and after the warp beam improvement were tested. The relevant parameters of the measured warp beam are listed in Table 1. The yarn type selected for the warp beam was slub yarn. Due to its yarn structure with periodically distributed thick and thin segments, slub yarn is more prone to noticeable tension fluctuations when the residual yarn of the warp beam is approximately 35% of the full beam. In addition, the actual production workshop frequently changes product varieties according to order requirements, making it difficult to obtain two warp beams with exactly the same number of warp yarns for a before-and-after comparison. Therefore, two production varieties with the same yarn material and similar varieties were selected for testing, with 363 and 385 warp yarns on the warp beam, respectively. It should be noted that the difference in the total number of warp yarns does not affect the tension characteristics of individual yarns.

3 Results and Discussion

3.1 Mechanism Analysis of Warp Yarn Fluctuation

The PID closed-loop tension control system is simulated and analyzed under the state of uniform unwinding speed. The values of the simulation parameters were carefully determined based on a comprehensive review of relevant standards, textbooks, and practical measurements[32,33]. The detailed parameter values are presented in Table 2. During the unwinding process, the moment of inertia of the warp beam can be unevenly distributed due to the eccentric warp beam. When the warp beam unwinding radius changes uniformly, the warp beam

Table 1 — Relevant parameters of the measured warp beam

Warp beam	Base yarn Count, Ne	Yarn type	Width, mm	Full beam radius, mm	Empty beam radius, mm	Number of warp yarns
WB-1	10	Slub yarn	1800	333	150	363
WB-2	10	Slub yarn	1800	331	150	385

Note: The warp yarns are all ring-spun cotton yarns.

winding density remains constant, the preset tension value is 120N, and the moment of inertia of the warp beam varies unevenly, the simulation results of the PID closed-loop control system for the warp yarn unwinding tension are shown in Fig. 5.

It can be seen from Fig. 5 that the tension fluctuation of the warp yarn gradually increases when the residual yarn of the warp beam is approximately 35% of the full beam. As the unwinding process proceeds, the warp beam unwinding radius and moment of inertia gradually decrease. However, the control parameters in the PID control system remain unchanged during the entire unwinding process. These constant control parameter settings make the system oscillate, resulting in warp yarn tension fluctuations. Moreover, under the same unwinding speed, a smaller warp beam radius results in a higher rotational speed, which further amplifies the effects of the uneven moment of inertia of the warp beam on tension and the frequency of external disturbances. Consequently, the frequency of change in the warp beam moment of inertia and the tension fluctuation will further increase significantly in this phase. For such fluctuations, the system must detect and respond to these disturbances in a very short time. Nevertheless, the PID control system often struggles to respond quickly and make timely adjustments, leading to reduced warp yarn tension stability and more pronounced oscillations.

In summary, the constant PID control parameters and the unevenness of the warp beam moment of inertia synergistically lead to the oscillation of the warp yarn tension control system and greater warp yarn tension fluctuations when the residual yarn of the warp beam is approximately 35% of the full beam, which affects the sizing quality and production efficiency.

Table 2 — Relevant parameters in the simulation

Parameters	Values
Friction coefficient β	0.07
Weight of empty warp beam G_0	180 kg
Distance between the flangesb	1800 mm
Initial radius of warp beam R_1	340 mm
Initial moment of inertia of warp beam J	17.66 kg·m^2
Barrel radius R_0	150 mm
Ruffle radius r_0	122.5 mm
Winding density of warp beam ρ	0.43 g/cm^3
Thickness of warp yarn (10S) h	0.0301 mm
Modulus of warp yarn E	2.06×10^9N/m^2
Cross-sectional area of warp yarn A	6.27×10^{-8} m^2
Distance between warp beam and guide roller L	1000 mm
Number of warp yarns n	400
Proportional coefficient of brake K_3	10
Relationship coefficient between tension and speed K_4	51665
Proportional coefficient of measuring device K_5	1

3.2 Simulation Analysis of Improvement Methods for Warp Yarn Fluctuation

3.2.1 Installation of Air Pressure Device

In the warp yarn unwinding tension control system, the actual tension is determined by the amount of regulated air pressure. When the tension error still exists after the control of the original system, it means that the amount of regulated air pressure is unreasonable. In the current production process, a unified multi-beam tension control method is generally used, which cannot achieve independent adjustment of individual beam tension. Therefore, an independent air pump and an air pressure proportional valve are installed. By utilizing the relationship between air pressure and tension, each warp beam can

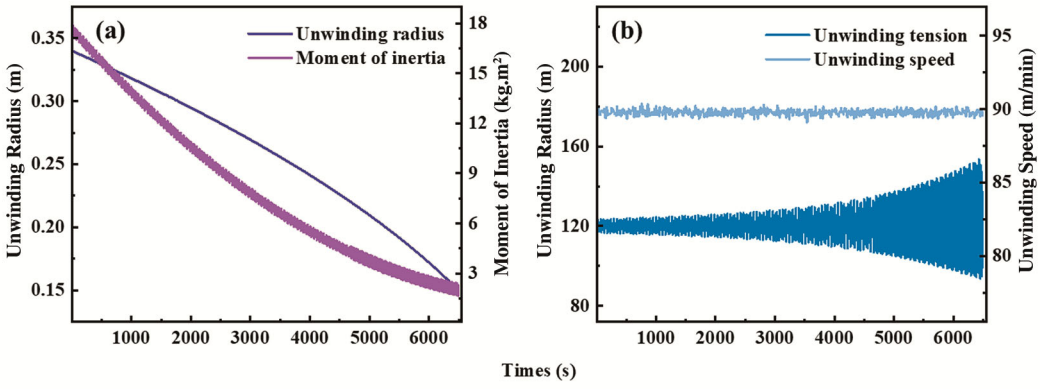

Fig. 5 — Simulation results of the PID closed-loop control system for the warp yarn unwinding tension: (a) unwinding radius and moment of inertia, and (b) unwinding tension and speed

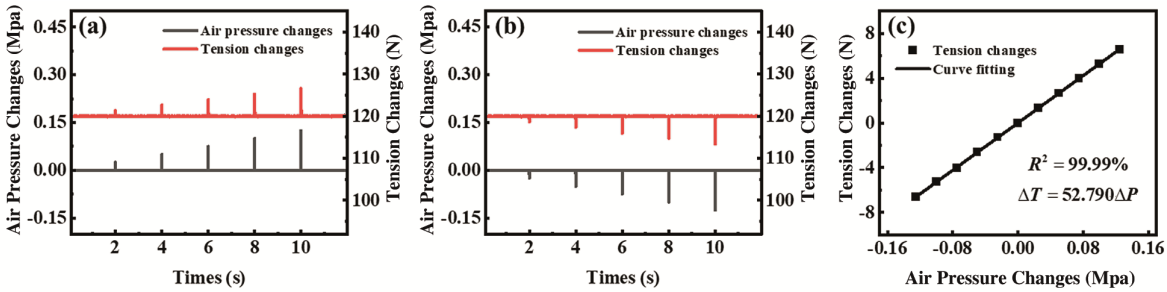

Fig. 6 — Simulation results of warp yarn tension change corresponding to additional air pressure regulation with T=120 N: (a) increase air pressure, (b) decrease air pressure, and (c) relationship between air pressure and tension

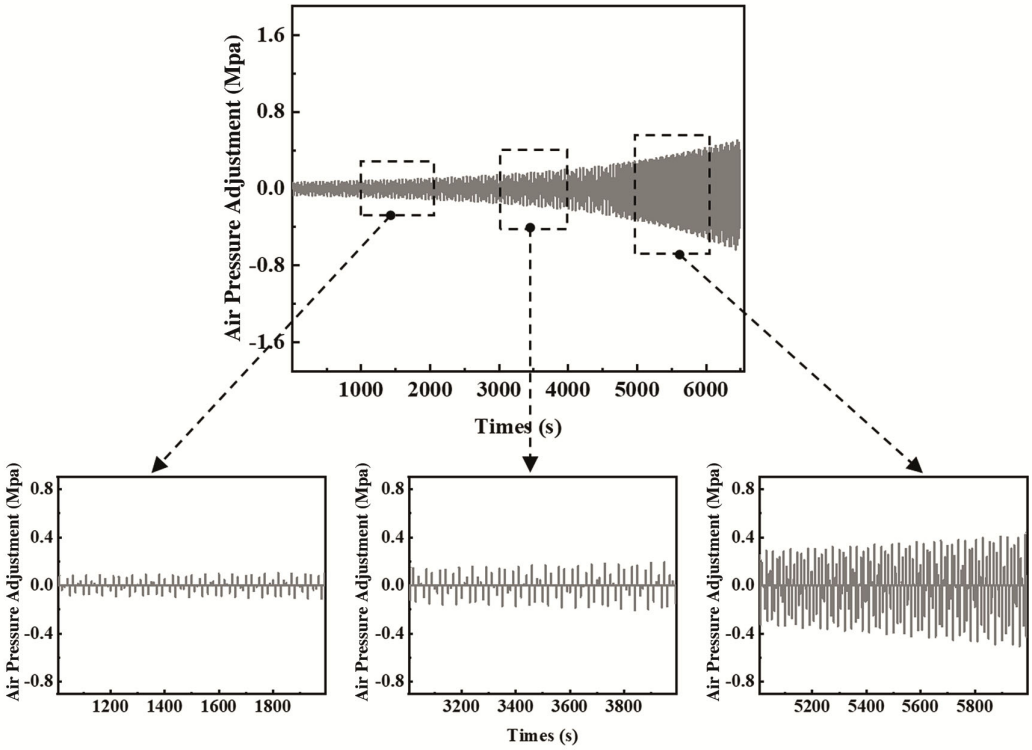

Fig. 7 — Additional air pressure compensation for the entire unwinding process

be independently regulated during unwinding, thereby promptly improving the warp yarn tension fluctuation due to system oscillation.

When the reference tension is 120N, the simulation results of the influence of independent air pressure adjustment on war p yarn tension are illustrated in Fig. 6. In Figs. 6(a) and (b), adding additional air pressure increases the warp yarn unwinding tension, while reducing air pressure decreases tension. Fig. 6(c) demonstrates the relationship between air pressure adjustmentΔP and tension changes ΔT, as shown in Eq. (15). The amount of additional air pressure is proportional to the change in tension, with proportional coefficients of 52.790.

$$\Delta T = 52.790\Delta P \quad \ldots(15)$$

According to the relationship between the additional air pressure adjustment and the tension, the warp yarn tension fluctuation during the unwinding process is regulated. When the warp yarn unwinding tension increases, indicating excessive air pressure provided by the system, the amount of additional air pressure is reduced. Conversely, when the tension decreases, additional air pressure is added to maintain constant tension.

Additional air pressure compensation throughout the entire unwinding process is illustrated in Fig. 7. The simulation results of additional air pressure regulating warp yarn tension fluctuation are shown in Fig. 8. Obviously, additional air pressure regulation

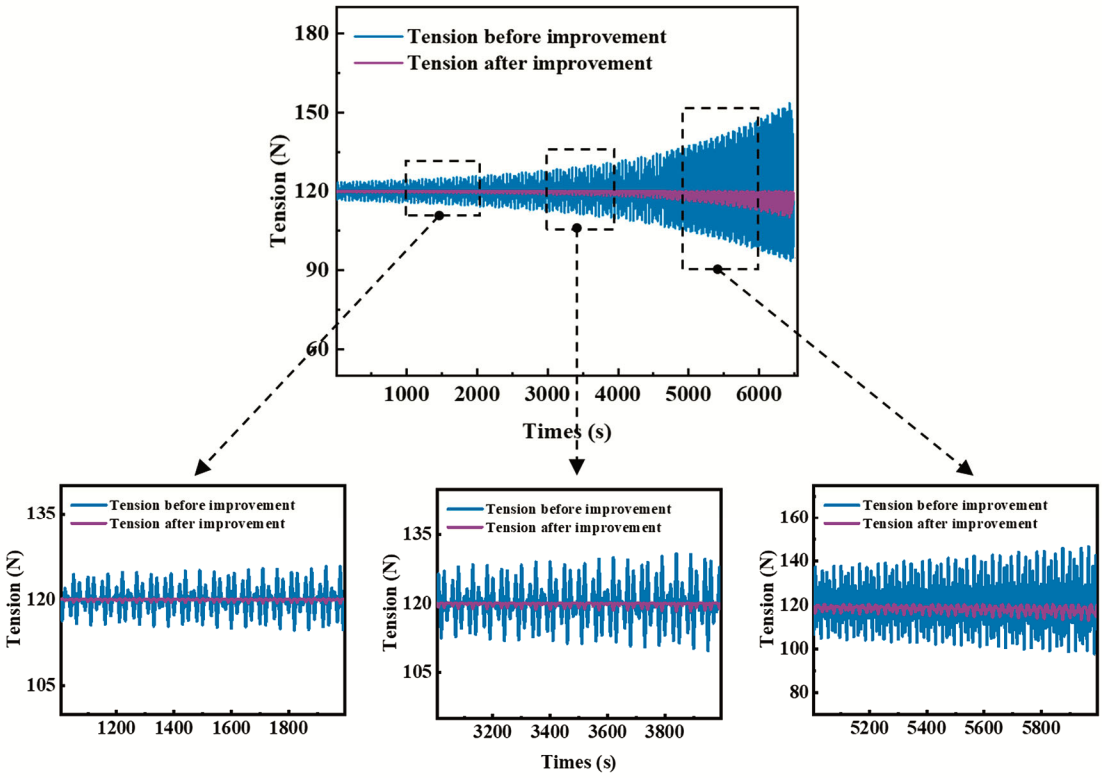

Fig. 8 — Changes in warp yarn unwinding tension before and after additional air pressure regulation

Table 3 — Change in warp yarn tension fluctuation before and after additional air pressure improvement

Warp beam	T_{fdmax}, N	T_{fdmin}, N	T_{fr}, N	$D_{rate-T_{fr}}$, %
Before improvement	33.431	26.329	59.760	83.16
After improvement	0.153	9.911	10.064	

Note: T_{pre} is the preset tension, T_{fdmax} and T_{fdmin} are the maximum and minimum tension fluctuation difference, T_{fr} is the tension fluctuation range, D_{rate} is the decrease rate. $T_{fdmax} = T_{max} - T_{pre}$, $T_{fdmin} = T_{pre} - T_{min}$, $T_{fr} = T_{fdmax} + T_{fdmin}$, $D_{rate-T_{fr}} = \frac{|T_{fr(After\ improvement)} - T_{fr(Before\ improvement)}|}{T_{fr(Before\ improvement)}} \times 100\%$

significantly improves warp yarn tension fluctuations during the entire unwinding process. In addition, the amplitude of additional air pressure adjustment increases proportionally with the magnitude of warp tension fluctuation.

Table 3 illustrates the change in warp yarn tension fluctuation before and after additional air pressure improvement. After the improvement, the warp yarn tension fluctuation range is reduced from 59.760 cN to 10.064 cN, which is reduced by 83.16%.

Thus, adding an additional air pressure device effectively mitigates the warp yarn tension fluctuation caused by system oscillation.

3.2.2 Segmented Control Method

The traditional closed-loop tension control method uses unified PID control parameters throughout the entire unwinding process. However, the warp beam unwinding radius and moment of inertia change all the time. In a nonlinear time-varying control system, the constant PID control parameters tend to have significant oscillations in the system when the residual yarn of the warp beam is approximately 35% of the full beam. Therefore, the whole warp beam is divided into large, medium and small warp beams based on diameter, and different PID control parameters are used for control. The PSO optimization algorithm is further used to tune the PID control parameters due to its simple structure, high optimization efficiency and accuracy[34-36].

Each particle represents a set of PID control parameter combinations, and its position and velocity are updated as follows:

Table 4 — Transfer functions of the warp beam

Warp beam	Time, s	R, mm	J, kg·m^2	Transfer function
Large warp beam	1360	310	12.66	$\frac{160161.5}{12.66s^2 + 19.06s + 0.105}$
Medium warp beam	3703	250	6.19	$\frac{129162.5}{6.19s^2 + 9.355s + 0.105}$
Small warp beam	5802	180	2.69	$\frac{92997}{2.69s^2 + 4.105s + 0.105}$

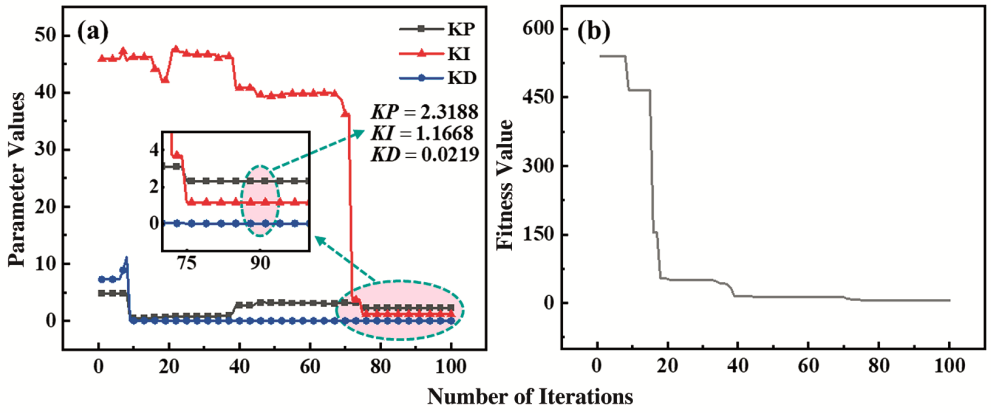

Fig. 9 — Change curves of PSO optimized PID parameters and fitness function for large warp beam: (a) $K_P/K_I/K_D$, and (b) fitness function

$$\begin{cases} V_{id}(k+1) = \omega \times V_{id}(k) + c_1 \times r_1 \times [p_{id}(k) - x_{id}(k)] \\ \quad +c_2 \times r_2 \times [p_{gd}(k) - x_{id}(k)] \\ x_{id}(k+1) = x_{id}(k) + V_{id}(k+1) \end{cases} \quad \ldots (16)$$

where $V_{id}(k)$ and $V_{id}(k+1)$ represent the velocity of particle i on the d dimension in the k and $k+1$ iteration, $x_{id}(k)$ and $x_{id}(k+1)$is called the position of particle i on the d dimension in the k and $k+1$ iteration, $p_{id}(k)$ and $p_{gd}(k)$ are the best historical position of particle i and the whole swarm of particles, respectively. ω denotes the inertia factor, $c_1$and c_2 are individual and group learning factors. r_1 and $r_2$are uniformly distributed random numbers between 0 and 1.

The fitness function BsJ(t) takes into account the output of the controller u(t), the output error e(t)and the rise time $t_u$of the control system, as shown in Eq. (17). In addition, when the output value yout(t)of the system decreases, the corresponding penalty term $100 \times |yout(t) - yout(t-1)|$is added to improve the system performance.

$$BsJ(t) = \int_0^t \left(0.999|e(t)| + 0.001u^2(t)\right) dt + 2t_u \quad \ldots (17)$$

The full beam radius of the warp beam is 340 mm. The unwinding radii of the large, middle and small warp beams are taken as 310mm, 250mm, and 180mm, respectively. According to the relevant simulation parameters and Eq. (7), the corresponding moment of inertia is obtained. Thus, transfer functions are presented in Table 4.

The large warp beam PSO-related parameters are $\omega = 0.6, c_1 = 1.7, c_2 = 2$, number of particles $n = 50$, number of iterations $z = 100$. Meanwhile, the PSO relevant parameters of the medium warp beam are $\omega = 0.6, c_1 = 1.4, c_2 = 1.6 n = 50, z = 100$. In addition, for the small warp beam, the PSO parameters are $\omega = 0.6, c_1 = 2.4, c_2 = 2.5, n = 50, z = 100$.

Figs. 9-11 show the change curves of PID control parameters ($K_P/K_I/K_D$) and corresponding fitness function after PSO optimization for the large, middle and small warp beams.Specifically, the control parameters of the large warp beam after optimization are $K_P = 2.3188$, $K_I = 1.1668$ and $K_D = 0.0219$.For the medium warp beam, the optimized control parameters are $K_P = 1.6328$, $K_I = 1.1178$and $K_D = 0.0158$. The optimized control parameters of the small warp beam are $K_P = 0.3006$, $K_I = 0.5480$ and $K_D = 0.0058$.

The optimized control parameters are used to control the warp yarn unwinding tension. When the

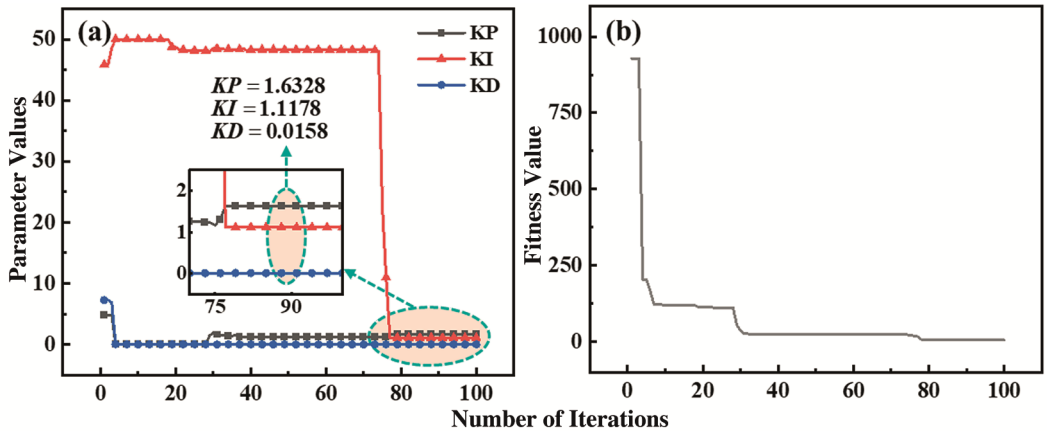

Fig. 10 — Change curves of PSO optimized PID parameters and fitness function for medium warp beam: (a) $K_P/K_I/K_D$, and (b) fitness function

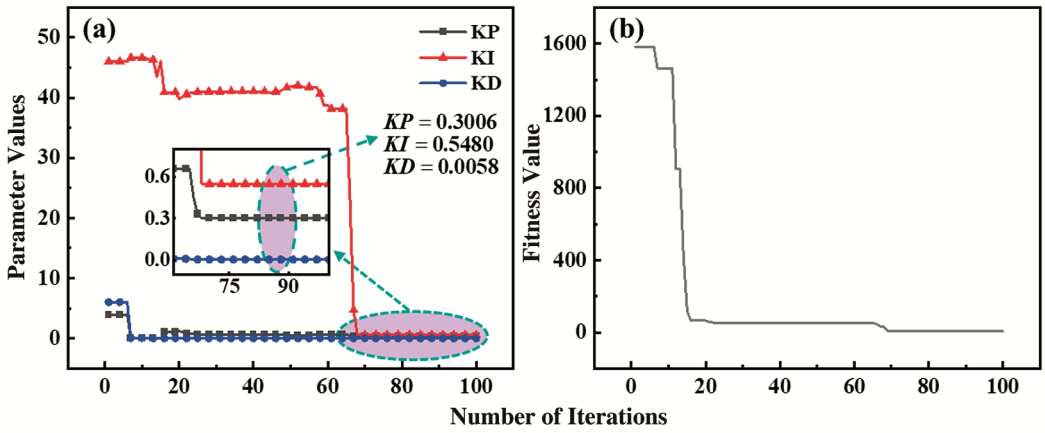

Fig. 11 — Change curves of PSO optimized PID parameters and fitness function for small warp beam: (a) $K_P/K_I/K_D$, and (b) fitness function

reference tension T=120N, the control effect of PSO-PID segmented control method in the steady-state stage is presented in Fig. 12. The PSO-PID segmented control method significantly improves the tension fluctuation during the entire unwinding process, and the control effect is better than PID control on large, medium and small warp beams.

Table 5 shows the change in warp yarn tension fluctuation before and after improvement of the PSO-PID segmented control method. The tension fluctuation range of the PSO-PID segmented control method is reduced by 89.44% compared with the PID control method. Hence, the PSO-PID segmented control strategy can be able to minimize the warp yarn tension fluctuation.

In conclusion, the simulation analysis reveals that the proposed methods of adding an independent air pressure device and the segmented control method have significantly improved the warp yarn tension fluctuation phenomenon when the residual yarn of the warp beam is approximately 35% of the full beam.

3.3 Experimental Verification

Based on the established models, we first have established the theoretical relationship between the decreased rate of speed and tension fluctuations range. When the tension is 120 N, the tension fluctuations at different unwinding speeds are shown in Fig. 13 and Table 6. It is evident that as the warp beam unwinding speed decreases, the tension fluctuation range of the warp beam unwinding diminishes. Since the higher the warp beam unwinding speed, the tension control system is more susceptible to factors such as unwinding radius and moment of inertia, resulting in an increased range of tension fluctuations.

Specifically, when the unwinding speed decreases by 13.36%, the corresponding tension fluctuation

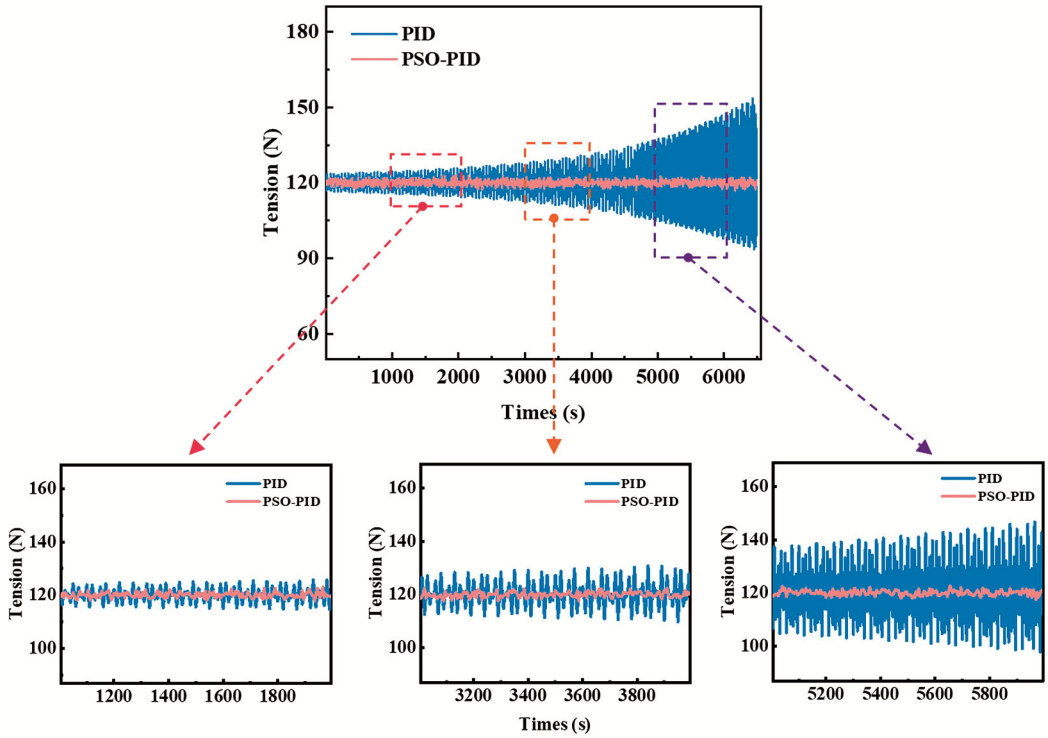

Fig. 12 — Control effect of PID and PSO-PID segmented control methods

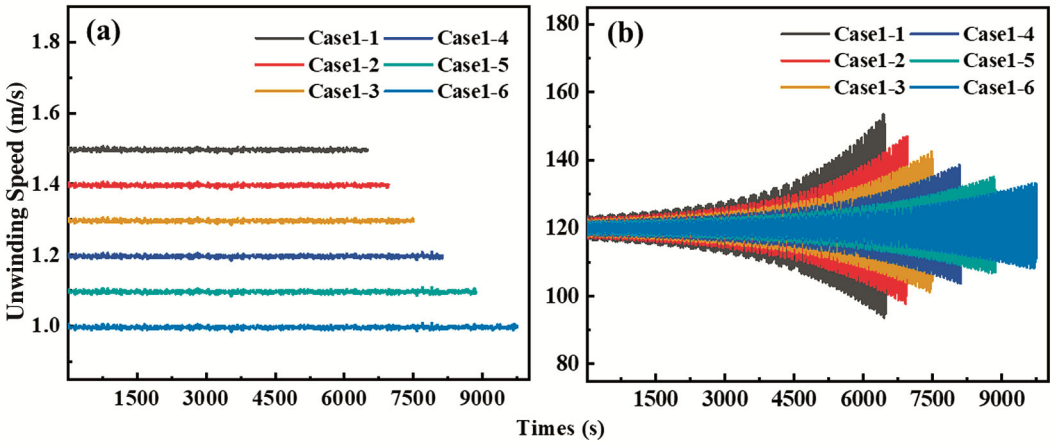

Fig. 13 — Simulation results of decreasing the unwinding speed to reduce tension fluctuation with T=120 N: (a) unwinding speed, and (b) unwinding tension

Table 5 — Change in warp yarn tension fluctuation before and after improvement of PSO-PID segmented control method

Warp beam	$T_{fdmax,}$N	$T_{fdmin,}$N	$T_{fr,}$N	$D_{rate-T_{fr.}}$%
PID	33.431	26.329	59.760	89.44
PSO-PID	3.086	3.222	6.308	

Note: $\mathbf{T_{pre}}$ **is** the preset tension, $\mathbf{T_{fdmax}}$ **and** T_{fdmin} are the maximum and minimum tension fluctuation difference, T_{fr} **is the** tension fluctuation range, D_{rate} **is the** decrease rate. $T_{fdmax} = T_{max} - T_{pre}$, $T_{fdmin} = T_{pre} - T_{min}$, $T_{fr} = T_{fdmax} + T_{fdmin}$, $D_{rate-T_{fr}} = \frac{|T_{fr(PSO-PID)} - T_{fr(PID)}|}{T_{fr(PID)}} \times 100\%$.

Table 6 — Tension fluctuation at different unwinding speeds with T=120 N

Case	V_2, m/s	V_1,m/s	T_{fdmax},N	T_{fdmin}, N	T_{fr}, N	D_{rate}, %	
						V_1	T_{fr}
Case1-1	1.5	1.496515	33.431	26.329	59.760	/	/
Case1-2	1.4	1.396515	26.902	22.190	49.092	6.68	17.85
Case1-3	1.3	1.296515	22.581	18.756	41.337	13.36	30.83
Case1-4	1.2	1.196515	18.595	16.230	34.825	20.05	41.73
Case1-5	1.1	1.096515	15.010	13.127	28.137	26.73	52.92
Case1-6	1.0	0.996515	13.136	11.783	24.919	33.41	58.30

Note: $T_{pre}$is the preset tension, $T_{fdmax}$and T_{fdmin} are the maximum and minimum tension fluctuation difference, T_{fr}isthe tension fluctuation range, D_{rate}isthe decrease rate. $T_{fdmax} = T_{max} - T$, $T_{fdmin} = T - T_{min}$, $T_{fr} = T_{fdmax} + T_{fdmin}$, $D_{rate-V_1} = \frac{|V_{1(Case1-n)} - V_{1(Case1-1)}|}{V_{1(Case1-1)}} \times 100\%$, n ∈ [2,6]. $D_{rate-T_{fr}} = \frac{|T_{fr(Case1-n)} - T_{fr(Case1-1)}|}{T_{fr(Case1-1)}} \times 100\%$, n ∈ [2,6].

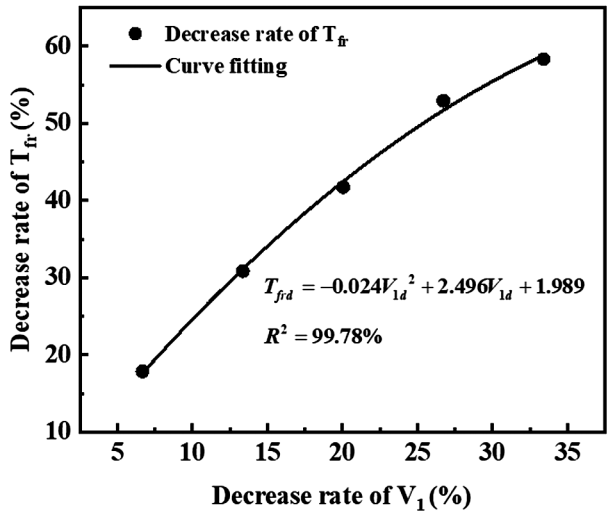

Fig. 14 — Relationship between the decreased rate of the unwinding speed and tension fluctuation range

range decrease rates reduce by 30.83%. The smaller the unwinding speed, the smaller the tension fluctuation range, but the longer the warp beam unwinding time. Therefore, it is appropriate to reduce the speed to minimize the tension fluctuation when the residual yarn of the warp beam is approximately 35% of the full beam by considering the output and production efficiency in actual production. The relationship between the decrease rate of unwinding speed and unwinding tension fluctuations range is shown in Fig. 14. This relationship follows a quadratic polynomial, as shown in Eq. (18). The fitted R^2 value is 99.78%.

$$T_{frd} = -0.024\,V_{1d}{}^2 + 2.469\,V_{1d} + 1.989 \quad \ldots (18)$$

where T_{frd} is the decrease rate of unwinding tension fluctuations range, $V_{1d}$is the decrease rate of unwinding speed.

Furthermore, experimental validation was carried out based on the constructed detection device. The changes in warp yarn tension and warp beam unwinding radius are illustrated in Fig. 15. As the unwinding process proceeds, the warp beam unwinding radius gradually decreases. Before improvement (WB-1), the average warp yarn unwinding speed was 90.75 m/min when running at a constant speed. As can be seen from Fig.15(a), the fluctuation of warp yarn tension increases significantly when the residual yarn of the warp beam is approximately 35% of the full beam, and even the phenomenon of 'loose yarn' occurs. Subsequently, the average warp yarn unwinding speed was reduced to 79.97 m/min, and the decrease rate was 11.88% (WB-2). In Fig. 15(b), both the duration and range of tension fluctuation are significantly reduced. Meanwhile, the occurrence frequency of abnormal conditions such as yarn breakage also decreases. Overall, the impact of the reduced speed on actual production efficiency is minimal compared with the improvement in tension stability.

Table 7 shows the relevant parameter changes. When the warp beam unwinding speed is reduced by 11.88%, the actual tension fluctuation range is reduced by 25.25%. The simulation parameters are consistent with the parameters related to the warp beam and warp yarn adopted in actual production. Therefore, the theoretical result of 28.25% was calculated using Eq. (18), which is basically in accordance with the experimental results.

In addition, the unwinding radius value of the initial oscillation before the warp beam unwinding decreases from 255.2 mm to 156.2 mm (with an empty beam radius of 150 mm), and the remaining yarn amount of the initial oscillation reduces from 48.23% to 2.18%.Meanwhile, during the entire

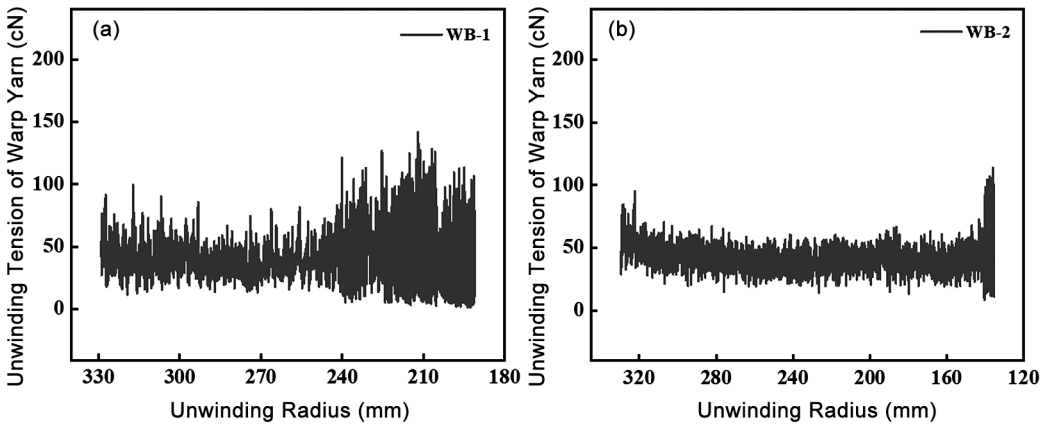

Fig. 15 — Changes in warp beam unwinding radius and warp yarn tension during uniform unwinding: (a) before improvement (WB-1), and (b) after improvement (WB-2)

Table 7 — Changes in relevant parameters before and after improvement

Warp beam	V_1, m/min	R_{io}, mm	Y_{ra}, %	T_{fr-act}, cN	T_{av}, cN	T_{cv}, %	D_{rate}, %		
							V_1	T_{fr-act}	T_{fr-the}
WB-1	90.75	255.2	48.23	140.6	42.09	47.07	11.88	25.25	28.25
WB-2	79.97	156.2	2.18	105.1	41.45	24.19			

Note: $R_{io}$is unwinding radius value of the initial oscillation, $Y_{ra}$is remaining yarn amount of the initial oscillation, $T_{fr-act}$and T_{fr-the}arethe actual and theoretical tension fluctuation range, $T_{av}$and $T_{cv}$are the average value and CV value of single warp yarn tension, $D_{rate-V_1} = \frac{|V_{1(WB-2)} - V_{1(WB-1)}|}{V_{1(WB-1)}} \times 100\%$, $D_{rate-T_{fr-act}} = \frac{|T_{fr(WB-2)} - T_{fr(WB-1)}|}{T_{fr(WB-1)}} \times 100\%$, $D_{rate-T_{fr-the}}$is calculated according to Eq. (18).

unwinding process, the average value and CV value of warp tension decreased from 42.09 cN and 47.07% to 41.45 cN and 24.19% respectively. That is, the warp tension CV value decreases by 22.88%. The tension fluctuation phenomenon has been significantly improved. Hence, the tension fluctuation when the residual yarn of the warp beam is approximately 35% of the full beam can be reduced by appropriately regulating the warp beam's unwinding speed, which can further balance the tension difference of the warp beam during the entire unwinding process.

In conclusion, the theoretical relationship between speed variation and tension fluctuation is consistent with the experimental results, further validating the accuracy of the established models of the warp yarn unwinding process and tension control system. Moreover, it demonstrates the effectiveness and feasibility of the proposed improvement methods based on model simulations.

4 Conclusion

This paper establishes mathematical models of the warp yarn unwinding process and tension control system. Based on these models, the mechanisms behind warp yarn tension fluctuations are clarified, and control system improvement methods are proposed and validated through simulations. Finally, the effectiveness of the established models and proposed methods is confirmed through experiments using constructed devices. The main conclusions are as follows:

(1) As the unwinding process proceeds, the unwinding radius and moment of inertia of the warp beam gradually decrease, while the rotational speed gradually accelerates. However, the constant yarn tension system control parameters and the uneven distribution of warp beam moment of inertia cause significant system oscillation when the residual yarn of the warp beam is approximately 35% of the full beam, further resulting in greater warp yarn tension fluctuations.

(2) The proposed improvement methods have good control effects to reduce the warp yarn tension fluctuation. Simulation analysis show that adding an independent air pressure device decreases the warp yarn tension fluctuation range by 83.16%. Simultaneously, the segmented control method reduces it by 89.44%.

(3) The relationship between the decreased rate of unwinding speed and warp yarn tension fluctuations

range follows a quadratic polynomial. In actual production, decreasing the warp beam unwinding speed by 11.88% results in a 25.25% reduction in the tension fluctuation range, which is consistent with the theoretical prediction of 28.25%. Thus, it further validates the reasonability of the proposed models and methods.

Therefore, the proposed mathematical modelling and improved control system offer a theoretical foundation and effective means for maintaining stable yarn tension in the sizing process, thereby contributing to enhanced sizing quality and fabric appearance uniformity. However, due to the structural complexity of existing sizing machines and the constraints of production scheduling, the proposed method still requires further validation under real production conditions. Future work will focus on evaluating its feasibility, robustness, and long-term stability in industrial applications, as well as exploring its potential extension to other textile processes.

References

1 Chowdhuri T, Kumar A, Kumar S, Saha S & Chattopadhyay D, *Indian J Fibre Text*, 50 (2025) 216.
2 Kabir S M F & Haque S, *J Nat Fibers*, 19 (2022) 6993.
3 Habtamu A & Ayele M, *J Nat Fibers*, 21 (2024) 2315513.
4 Ling Y L, Chen M T, Liu Y & Yin R, *Fibers Polym*, 24 (2023) 2967.
5 Eren R, Kilic S & Atalay Ö, *J Eng Fiber Fabr*, 20 (2025) 1.
6 Ayele M & Abay A G, *J Nat Fibers*, 20 (2023) 2165591.
7 Xu H Y, *J Text Res*, 18 (1997) 63.
8 Gao W D, Jiang W M, Wang J A & Wang W C, *Cotton Text Tech*, 51 (2023) 41.
9 Wei Z D, Xu H C & Su H, *Appl Mech Mater*, 397 (2013) 409.
10 Sun C L & Qiu J W, *J Text Res*, 13 (1992) 46.
11 Zhang R G, Feng P & Yang C C, *Text Res J*, 92 (2022) 4587.
12 Jang J S, Kim K W, Kang J H, Park H G, Cho Y J & Lee J W, *Nonlinear Dynam*, 100 (2020) 3199.
13 Hu X T, Zhang Y J, Meng Z & Sun Y Z, *J Text Res*, 38 (2017) 111.
14 Matsushita S, Kuromiya A, Takagi K, Furuhashi T, Horikawa S & Uchikawa Y, *IEEJ Trans Ind Appl*, 114 (1994) 1012.
15 Peng Z H, Ma G & Zhou C, *J Text Res*, 32 (2011) 127.
16 Turukmane R, Gulhane S & Patil R B, *Melliand China*, 48 (2020) 10.
17 Zhang H P, *J Text Res*, 3(1982) 29.
18 Hu G L, *Beijing Text J* , (1987) 17.
19 Chen J R & Zhou J C, *Jiangsu Text*, (1994) 45.
20 Ru Y J, Huang S K, Huang X P & Gao T L, *Shanghai Text Sci Tech*, (1982) 11.
21 Wang L, Wang H S, Ouyang Z, Liu H & Zheng Z X, *IEEE Access*, 12 (2024) 103660.
22 Zhang H, Xia H D, Lu Y F, Wu J, Zhang X H & Wei Y K, *Text Res J*, 92 (2022) 5049.
23 Wang L, Peng L, Xiong X, Hu X, Sun L & Li Y, *Text Res J*, 95 (2025) 850.
24 Xue Z C, *Cotton Text Tech*, 37 (2009) 373.
25 Tong Y, *Adv Mater Res*, 1049 (2014) 908.
26 Li L, Yang J C, Zhao Y L, Liu Y & Cong L C, *Proc ICICTA Conf*, (2010).
27 Liu S G & Wei J M, *J Text Res*, 15 (1994) 4.
28 Liu S G & Luo B. T, *ICISE*(2009).
29 Tu L, Guo M R, Wang J A & Gao W D, *Text Res J*, 94 (2024) 1126.
30 Zhang Q, Wang S L, Zhang A R, Zhou J & Liu Q, *Control Eng Pract*, 67 (2017) 31.
31 Chen P, Cheng Y, Yuan Y L & Hua L, *T I Meas Control*, (2024).
32 *Textile machinery and accessories-Beams for winding-Part 2: Warper's beams* IS: 8116-2 (International Organization for Standardization, Switzerland), (2008).
33 Zhu S K&Gao W D, *Weaving technology* (ChinaTextile & Apparel Press, Beijing), (2008)64.
34 Xu M D, Wang Z C, Niu X J, Wang Z, Zou W, Zhai C Y & Li S, *Agriculture*, 16 (2026) 481.
35 Mustafa N & Hashim F H, *Inter J Electron Telec*, 66 (2020) 737.
36 Zhu D, Li R, Zheng Y, Zhou C, Li T & Cheng S, *Arch Comput Method E*, 32 (2025) 1571.